Acta Crystallographica Section D
Biological Crystallography
ISSN 0907-4449

Human phosphoglucose isomerase: expression, purification, crystallization and preliminary crystallographic analysis

Artur T. Cordeiro,[a] Paulo H. C. Godoi,[a,b] Luis F. Delboni,[a]† Glaucius Oliva[a,b] and Otavio H. Thiemann[a]*

[a]Laboratory of Protein Crystallography and Structural Biology, Physics Institute of São Carlos, University of São Paulo - USP, Av. Trabalhador Sãocarlense 400, PO Box 369, 13566-590 São Carlos - SP, Brazil, and [b]Chemistry Institute of São Carlos - USP, Av. Trabalhador Sãocarlense 400, PO Box 369, 13566-590 São Carlos - SP, Brazil

† Present address: Pontificia Universidade Católica de Poços de Caldas, MG, Brazil.

Correspondence e-mail: thiemann@if.sc.usp.br

Received 2 October 2000
Accepted 16 January 2001

Phosphoglucose isomerase (PGI) is the second enzyme in the glycolytic pathway and catalyzes an aldose–ketose isomerization. Outside the cell, PGI has been found to function as both a cytokine and as a growth factor. The human *pgi* gene was cloned and the expressed enzyme was purified to homogeneity. Isomorphous crystals were obtained under two conditions and belong to the $P2_12_12_1$ space group, with unit-cell parameters $a = 80.37$, $b = 107.54$, $c = 270.33$ Å. A 94.7% complete data set was obtained and processed to a limiting resolution of 2.6 Å. The asymmetric unit contains two hPGI dimers according to density calculations, a self-rotation function map and molecular-replacement solution.

1. Introduction

Phosphoglucose isomerase (PGI; E.C. 5.3.1.9) is a multifunctional enzyme composed of homodimers with molecular masses ranging from 100 to 120 kDa. With the exception of some intracellular parasites, PGIs are involved in the glycolytic and gluconeogenesis pathways in most known organisms (Andersson *et al.*, 1998). PGIs catalyze the intracellular isomerization reaction of D-glucose-6-phosphate (G6P) to D-fructose-6-phosphate (F6P). The proposed catalytic mechanism involves several steps *via* the formation of a *cis*-enediol intermediate, similar to triose phosphate isomerase.

The sequence similarity between PGIs and neuroleukin (NL; Faik *et al.*, 1988), autocrine motility factor (AMF; Li & Chirgwin, 2000) and differentiation and maturation mediator (DMM; Xu *et al.*, 1996) indicates a broader role for this enzyme in cell function. Recent investigation has shown the stimulation of mouse tumour cells' motility and the enhancement of neurite outgrowth in progenitors of neuronal cells by the addition of *Bacillus stearothermophilus* PGI to the culture medium (Sun *et al.*, 1999).

The human homologue hPGI and its isoenzymes have been purified from several tissues with no particular tissue specificity. hPGI has been characterized by the analysis of human genetic defects affecting the *pgi* gene (Xu & Beutler, 1994). Defects in the *hpgi* loci are the cause of many autosomal recessive disorders such as haemolytic anaemia. Depending on the severity of the PGI deficiency, neonatal death can occur from neurological disorders.

The crystallographic structures of the rabbit, *Bacillus* and pig PGI enzymes have been previously reported at resolutions ranging from 2.3 to 6.0 Å (Jeffery *et al.*, 2000; Hsiao *et al.*, 1997; Muirhead & Shaw, 1974). Although the sequence similarity of hPGI, cytokines and growth factors reveal a broader enzyme function, no structural data has been obtained for the human enzyme. The availability of a crystal structure of hPGI could help elucidate the enzyme catalytic mechanism and its substrate specificity. We present here the first successful expression, crystallization and preliminary X-ray characterization of the human PGI enzyme. The data obtained shows that the hPGI enzyme crystallizes in conditions similar to those of the rabbit homologue (Jeffery *et al.*, 2000).

2. Materials and methods

2.1. Human PGI expression, purification and characterization

The *hpgi* gene was amplified from a human brain cDNA library (GIBCO-BRL) by the polymerase chain reaction (PCR) based on the available human PGI sequence (accession No. NM_000175). Oligodeoxynucleotide primers for PCR amplification (GIBCO-BRL) introduce both *Nde*I and *Hin*dIII restriction sites at the 5′ and 3′ end, respectively (5′-AGAGCTCC**CATATG**GCCGCTCTCACCCGGGAC-3′, *Nde*I; 5′-AGCT**AAGCTT**TTATTGGACTCTGGCCTCGCGC-3′, *Hin*dIII) for cloning into the pET29a(+) expression vector (Novagen). The PCR reaction, containing 2 pmol of each primer and approximately 50 ng of the human brain cDNA, was carried out in a GeneAmp 2400 thermocycler (Perkin-Elmer CETUS) with 2.5 U of AmpliTaq DNA polymerase (Promega) according to the manufacturer's instructions. The sample was subjected to 2 min denaturation at 367 K followed by 30 cycles of denaturation at 367 K for 0.5 min, annealing at 313 K for 0.5 min and extension at

345 K for 1 min. A DNA band of approximately 1.8 kbp in length was gel purified by the NaI glass powder method (Vogelstein & Gillespie, 1979). The purified DNA was digested with the restriction enzymes *Nde*I and *Hind*III, subcloned into the pET29a(+) vector and transformed into BL21(DE3) competent cells. The cloned *hpgi* was sequenced in an ABI377 DNA sequencer to confirm its sequence identity. Cells from a single colony were grown overnight at 310 K, 250 rev min^{-1} in 5 ml LB medium containing 50 µg ml^{-1} kanamycin. A larger cell culture was grown in 2×YT with 25 µg ml^{-1} kanamycin at 310 K, 250 rev min^{-1} until OD_{600} = 0.6. The culture was then induced for 4 h with 0.5 m*M* IPTG.

The *E. coli* BL21(DE3) cells were harvested by centrifugation at 4000*g* for 30 min. The cell pellet was suspended in 20 ml of 50 m*M* Bicine pH 7.8 (buffer *A*) and cell lysis was obtained by adding lysozyme (0.5 mg ml^{-1}) and repeated cycles of freeze–thawing. The crude extract was clarified by centrifugation (6000*g*, 10 min) and brought to 50%(*w*/*v*) ammonium sulfate for 20 min with slow shaking. The suspension was separated by centrifugation for 15 min at 20 000*g*, 277 K and subjected to a second precipitation step in 80%(*w*/*v*) ammonium sulfate as described above. The protein pellet was solubilized in 9 ml buffer *A* and dialyzed against 250 ml of the same buffer with two buffer exchanges. The hPGI from the 50–80% fraction was loaded onto a 16 ml SP Sepharose-HP column equilibrated with buffer *A*. The hPGI eluted at approximately 1.3 *M* NaCl in a linear gradient of buffer *B* (buffer *A* plus 2 *M* NaCl). hPGI was dialyzed against 50 m*M* Bicine, 150 m*M* NaCl pH 7.8 and applied to a 115 ml Superdex-200 column equilibrated with 50 m*M* Bicine, 150 m*M* NaCl pH 7.8. The human PGI solution was concentrated by ultrafiltration using Centriprep 30 and Centricon 10 (Millipore) to 8 mg ml^{-1} in 12.5 m*M* Bicine pH 7.5, 37.5 m*M* NaCl. The isoelectric point for the recombinant hPGI was determined by gel isoelectric focusing in the pH range 3–9 (PHAST system, Pharmacia). The kinetic parameters K_m and V_{max} were measured at room temperature following the formation of NADPH at 340 nm for 1 min (Gracy & Tilley, 1975).

2.2. Crystallization, diffraction data collection, processing and initial phasing

The crystallization conditions for the hPGI protein were initially screened by the hanging-drop vapour-diffusion method using the sparse-matrix kits Crystal Screen 1 and 2 from Hampton Research at 277 and 291 K. A solution of 3 µl hPGI protein containing 8 mg ml^{-1} enzyme in 12.5 m*M* Bicine pH 7.5, 37.5 m*M* NaCl was mixed with an equal volume of the Crystal Screen 1 and 2 well solutions (500 µl per well) to form the drop. Screening different concentrations of precipitating agent and pH further optimized the initial crystallization conditions.

The best crystallization condition for the hPGI was obtained at 291 K in droplets consisting of 3 µl of protein solution at 8 mg ml^{-1} in the buffer described above and 3 µl of reservoir solution. The reservoir solution (500 µl) contained 10% PEG 10 000, 100 m*M* HEPES pH 7.5.

Diffraction data were collected on an R-AXIS IIC image-plate detector mounted on a Rigaku RU200B rotating-anode generator operating with a copper target at 50 kV and 100 mA. Crystals were mounted in nylon loops (Hampton Research) after quick soaking in a cryoprotectant solution consisting of the same reservoir solution and 20% MPD. A total of 79 frames were collected using the oscillation method. Individual frames consisted of 1° oscillation and 30 min exposure at a crystal-to-detector distance of 130 mm. The data were processed using *DENZO* and *SCALEPACK* from the *HKL* suite (Otwinowski & Minor, 1997). The Matthews coefficient and solvent content were calculated with the program *MATTHEWS_COEFF*. The self-rotation function was calculated using *AMoRe* (Navaza, 1997) and *GLRF* (Tong, 1997) in the resolution range 15–3.5 Å with an integration radius of 25 Å. The Patterson map was calculated using *CNS* (Brunger *et al.*, 1998) with 35–2.6 Å resolution data.

Initial phasing was obtained by molecular replacement using *AMoRe* (Navaza, 1997) and the dimeric rabbit PGI structure as model (PDB code 1dqr) at 2.5 Å. The search for the rotation and translation functions was performed using data in the resolution range 15–3.5 Å from the hPGI data set, equivalent to 28 025 reflections.

3. Results and discussion

The availability of large quantities of pure protein is of paramount importance for biophysical studies and especially for crystallographic structure determination. The structures of PGI from *B. stearothermophilus* (Hsiao *et al.*, 1997) and more recently the rabbit phosphoglucose isomerases (rPGI) have been determined (Jeffery *et al.*, 2000). In spite of the intense investigation of this multifunctional enzyme, no structural data has been reported for the human homologue. Starting from a human brain cDNA library, the procedure leading to the expression, purification, crystallization and preliminary crystallographic analysis of human PGI is described.

The recombinant hPGI protein was overexpressed and purified to homogeneity by a three-step purification protocol. Spectrophotometric assays and electrophoresis followed the purity of the sample. On a 15% SDS–PAGE, the purified hPGI protein migrates as a single band of about 60 kDa (Fig. 1*a*) corresponding to the expected hPGI monomer (Carter & Yoshida, 1969). The relative molecular size determined from size-exclusion chromatography showed that the recombinant hPGI elutes as a homodimer of 120 kDa, as previously reported for other PGI enzymes (Carter & Yoshida, 1969) (data not shown).

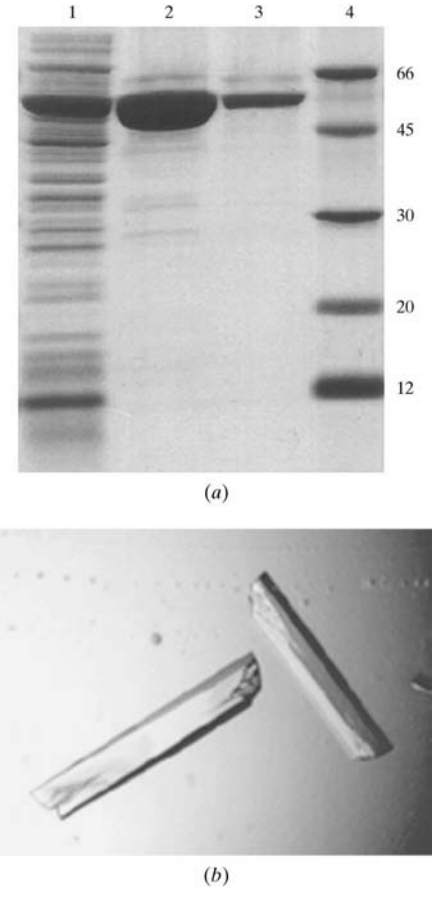

Figure 1
Purification and crystallization of human PGI. (*a*) SDS–PAGE analysis of hPGI purification results. Lane 1, protein pellet after 50–80% ammonium sulfate fraction; lane 2, eluted fraction from SP Sepharose-HP column; lane 3, eluted fraction after Superdex-200; lane 4, molecular-weight markers (kDa). (*b*) Human PGI crystals obtained in 10% PEG 10 000, 100 m*M* HEPES pH 7.5 at 291 K by the hanging-drop vapour-diffusion technique. The lower left crystal has approximate dimensions of 0.1 × 0.1 × 0.6 mm.

Table 1
Comparison between hPGI and rPGI crystallization conditions and crystal characteristics.

	hPGI	rPGI
Crystallization conditions	10% PEG 10 000, 100 m*M* HEPES pH 7.5	13% PEG 8000, 250 m*M* Mg acetate, 100 m*M* Na cacodylate pH 6.5
Space group	$P2_12_12_1$	$C222_1$
Unit-cell parameters (Å)		
a	80.37	82.69
b	107.54	115.27
c	270.33	271.84
Matthews coefficient (Å^3 Da^{-1})	2.68	2.41
Solvent content (%)	53.70	48.64

The expression and purification protocol described here allowed the recovery of approximately 5 mg of pure recombinant hPGI enzyme, with an enzymatic specific activity of 440 U mg^{-1}. The kinetic parameters of hPGI were analysed and a K_m value of 96 m*M* for F6P and a V_{max} of 21 m*M* min^{-1} were obtained, indicating that the recombinant hPGI enzyme is appropriate for crystallographic analysis and represents well the wild-type enzyme.

The hPGI protein was crystallized as described in §2. The best condition (10% PEG 10 000, 100 m*M* HEPES pH 7.5) resulted in the formation of rectangular-shaped crystals of approximately 0.1 × 0.1 × 0.6 mm dimensions after one week at 291 K. The crystals belong to the orthorhombic space group $P2_12_12_1$, with unit-cell parameters a = 80.37, b = 107.54, c = 270.33 Å (Fig. 1*b*). Statistical analysis of the merged reflections indicated that the collected data set is better described as having a limiting resolution of 2.6 Å, with a total of 147 487 recorded reflections merged to 69 187 unique reflections. The overall completeness and R_{merge} correspond to 94.7 and 9.9%, respectively, and in the last shell 95.6 and 28.5%, respectively. Assuming two dimers in the asymmetric unit, the calculated Matthews coefficient is 2.41 Å^3 Da^{-1} (Matthews, 1968). A solvent content of 48.64% was obtained considering a protein density of 1.34 g cm^{-3}.

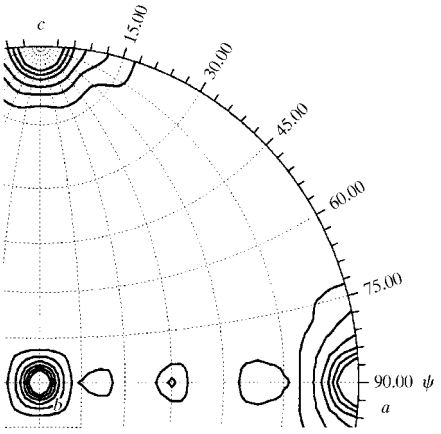

Figure 2
Preliminary crystallographic analysis. Stereographic projection of κ = 180° section of the self-rotation function map of hPGI limited to polar angles φ = 0–105, ψ = −105° contoured at 0.6σ as calculated with the program *GLRF*.

The self-rotation function analysis showed the presence of a single non-crystallographic twofold axis with a peak correlation coefficient of 30%. The peak is at Eulerian angles α = 42.5, β = 172.5, γ = 42.5°, corresponding to a twofold rotation axis approximately parallel to the unit-cell *ab* plane and at an angle of 45° to the *a* axis. Other peaks were observed with a lower height and no symmetry axis could be associated with them; therefore, we considered these to be spurious peaks. The twofold rotation axis relates one molecule of the dimer to the other, representing a intra-dimer twofold axis. These results were confirmed by *GLRF* (Tong, 1997). The stereographic projection of section χ = 180°, represented in Fig. 2, shows the three crystallographic axes along *a*, *b* and *c* and a single non-crystallographic axis between axes *a* and *b*.

The molecular-replacement studies using the dimeric rabbit PGI (rPGI) as the search model, having 92% sequence identity to hPGI, indicated a solution for the rotation and translation functions with two dimers in the asymmetric unit. A final correlation coefficient of 68.8% was found, which was well above the remaining peaks. The observed positions for the four independent hPGI molecules in the asymmetric unit are in agreement with the expected twofold non-crystallographic axis as seen by *GLRF* and *AMoRe*.

The molecules are organized as two independent dimers identically oriented and related by a translation of (0.5, 0.5, 0.134) in fractional coordinates along the cell axes. The calculated Patterson map shows a strong peak associated with those coordinates. This peak is 17.6% of the height of the origin peak, corresponding to a 75σ level, and is the only significant peak in the whole map apart from the origin.

Comparing the rPGI and hPGI proteins, many similarities can be observed with respect to their crystallization conditions, unit-cell parameters, Matthews coefficient and solvent content (Table 1). As a consequence, the same number of molecules in the unit cell are expected, though in a somewhat different arrangement since the proteins crystallized in different space groups: $C222_1$ for rPGI and $P2_12_12_1$ for hPGI. Indeed, in the rabbit PGI crystal, two dimers are related by the exact crystallographic *C*-centring operation, whereas in the human PGI crystal two dimers are related by a non-crystallographic translation (Figs. 2 and 3).

Finally, the successful crystallization of human PGI enzyme suitable for structure determination should allow us to answer many of the fundamental questions that remain unclear about the mechanisms of

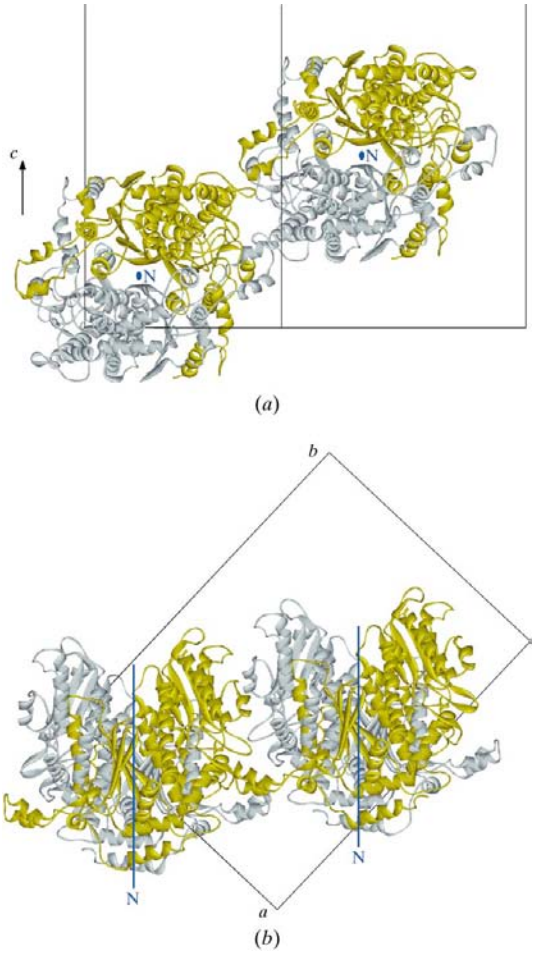

Figure 3
Ribbon representation of the two independent hPGI dimers in the crystal unit cell. (*a*) View down the non-crystallographic twofold axis relating the monomers in each dimer; (*b*) view down the crystal *c* axis. '*N*' (in blue) indicates a single non-crystallographic axis between axes *a* and *b*.

catalysis and of its multifunctional activity. We are currently refining the molecular-replacement solution.

This work was supported in part by a research grant 98/14979-7 to OHT (FAPESP). GO is an International Scholar of the Howard Hughes Medical Institute. ATC and PHCG are FAPESP student fellowship awardees. We would like to thank the members of the Protein Crystallography and Structural Biology Group (IFSC-USP) for helpful discussions in the course of this work and to express our gratitude to Dr Flávio H. Silva (DGE-UFSCar) for making available the Human Brain cDNA library used in this study.

References

Andersson, S. G., Zomorodipour, A., Andersson, J. O., Sicheritz-Ponten, T., Alsmark, U. C., Podowski, R. M., Naslund, A. K., Eriksson, A. S., Winkler, H. H. & Kurland, C. G. (1998). *Nature (London)*, **396**, 133–140.

Brunger, A. T., Adams, P. D., Clore, G. M., DeLano, W. L., Gros, P., Grosse-Kunstleve, R. W., Jiang, J. S., Kuszewski, J., Nilges, M., Pannu, N. S., Read, R. J., Rice, L. M., Simonson, T. & Warren, G. L. (1998). *Acta Cryst.* D**54**, 905–921.

Carter, N. D. & Yoshida, A. (1969). *Biochim. Biophys. Acta*, **181**, 12–19.

Faik, P., Walker, J. I., Redmill, A. A. & Morgan, M. J. (1988). *Nature (London)*, **332**, 455–457.

Gracy, R. W. & Tilley, B. E. (1975). *Methods Enzymol.* **41**, 392–400.

Hsiao, C. D., Chou, C. C., Hsiao, Y. Y., Sun, Y. J. & Meng, M. (1997). *J. Struct. Biol.* **120**, 196–200.

Jeffery, C. J., Bahnson, B. J., Chien, W., Ringe, D. & Petsko, G. A. (2000). *Biochemistry*, **39**, 955–964.

Li, X. & Chirgwin, J. M. (2000). *Biochim. Biophys. Acta*, **1476**, 363–367.

Matthews, B. W. (1968). *J. Mol. Biol.* **33**, 491–497.

Muirhead, H. & Shaw, P. J. (1974). *J. Mol. Biol.* **89**, 195–203.

Navaza, J. (1997). *Methods Enzymol.* **276**, 581–594.

Otwinowski, Z. & Minor, W. (1997). *Methods Enzymol.* **276**, 307–326.

Sun, Y. J., Chou, C. C., Chen, W. S., Wu, R. T., Meng, M. & Hsiao, C. D. (1999). *Proc. Natl Acad. Sci. USA*, **96**, 5412–5417.

Tong, L. (1997). *Methods Enzymol.* **276**, 594–611.

Vogelstein, B. & Gillespie, D. (1979). *Proc. Natl Acad. Sci. USA*, **76**, 615–619.

Xu, W. & Beutler, E. (1994). *J. Clin. Invest.* **94**, 2326–2329.

Xu, W., Seiter, K., Feldman, E., Ahmed, T. & Chiao, J. W. (1996). *Blood*, **87**, 4502–4506.